5 August 1996

PHYSICS LETTERS A

ELSEVIER

Physics Letters A 218 (1996) 255–267

Multiband strange nonchaotic attractors in quasiperiodically forced systems

O. Sosnovtseva [a,b], U. Feudel [a,c], J. Kurths [a], A. Pikovsky [a]

[a] *Max-Planck-Arbeitsgruppe "Nichtlineare Dynamik", Potsdam Universität, Potsdam, Germany*

[b] *Department of Physics, Saratov State University, Saratov, Russian Federation*

[c] *Institute of Plasma Research, University of Maryland, College Park, MD, USA*

Received 28 July 1995; revised manuscript received 1 April 1996; accepted for publication 3 May 1996
Communicated by C.R. Doering

Abstract

We study the effect of quasiperiodic forcing on two-dimensional invertible maps. As basic models the Hénon and the ring maps are considered. We verify the existence of strange nonchaotic attractors (SNA) in these systems by two methods which are generalized to higher dimensions: via bifurcation analysis of the rational approximations, and by calculating the phase sensitivity. Analyzing these systems we especially find a new phenomenon: the appearance of strange nonchaotic attractors which consist of 2^n bands. Similar to the band-merging crisis in chaotic systems, such a 2^n band SNA can merge to a 2^{n-1} band SNA.

1. Introduction

In nonlinear dynamical systems strange attractors are considered as structures in phase space that usually correspond to chaotic behavior. Ten years ago Grebogi, Ott, Pelikan and Yorke [1] showed that in a certain type of dynamical systems there are attractors which are strange but not chaotic. These strange nonchaotic attractors (SNA) are strange in a geometrical sense, i.e. they are fractals. On the other hand, they show no sensitive dependence on initial conditions, therefore, they are not chaotic. Not only their strange structure with nonchaotic dynamics but also their unusual spectral and correlation properties characterize them as important structures between regular (here quasiperiodic) and chaotic motion [2]. SNAs have been found in different model systems: in maps, such as the quasiperiodically forced circle and logistic maps [3–5], as well as in continuous-time systems, such as the damped pendulum [6,7] and the Duffing oscillator [8]. They have been related to Anderson localization in the Schrödinger equation with a spatially quasiperiodic potential [9]. SNA have been also observed experimentally in a quasiperiodically forced magneto-elastic ribbon [10] and in an oscillator with a multistable potential [11]. For all these systems it is common that SNAs occur when a quasiperiodic forcing is applied. Generally, in systems with quasiperiodic forcing the following bifurcation sequence can be observed: Firstly, a smooth torus is destroyed and an SNA appears. Secondly, a transition to chaos happens.

In this paper we study the properties of SNA from the point of view of such a transition. We mainly focus on the mechanisms of the appearance of SNA and their possible further transitions. As the basic models we investigate the ring and the Hénon maps with quasiperiodic forcing. Contrary to the other systems studied recently [3–5], we consider here diffeomorphisms,

PII S0375-9601(96)00399-4

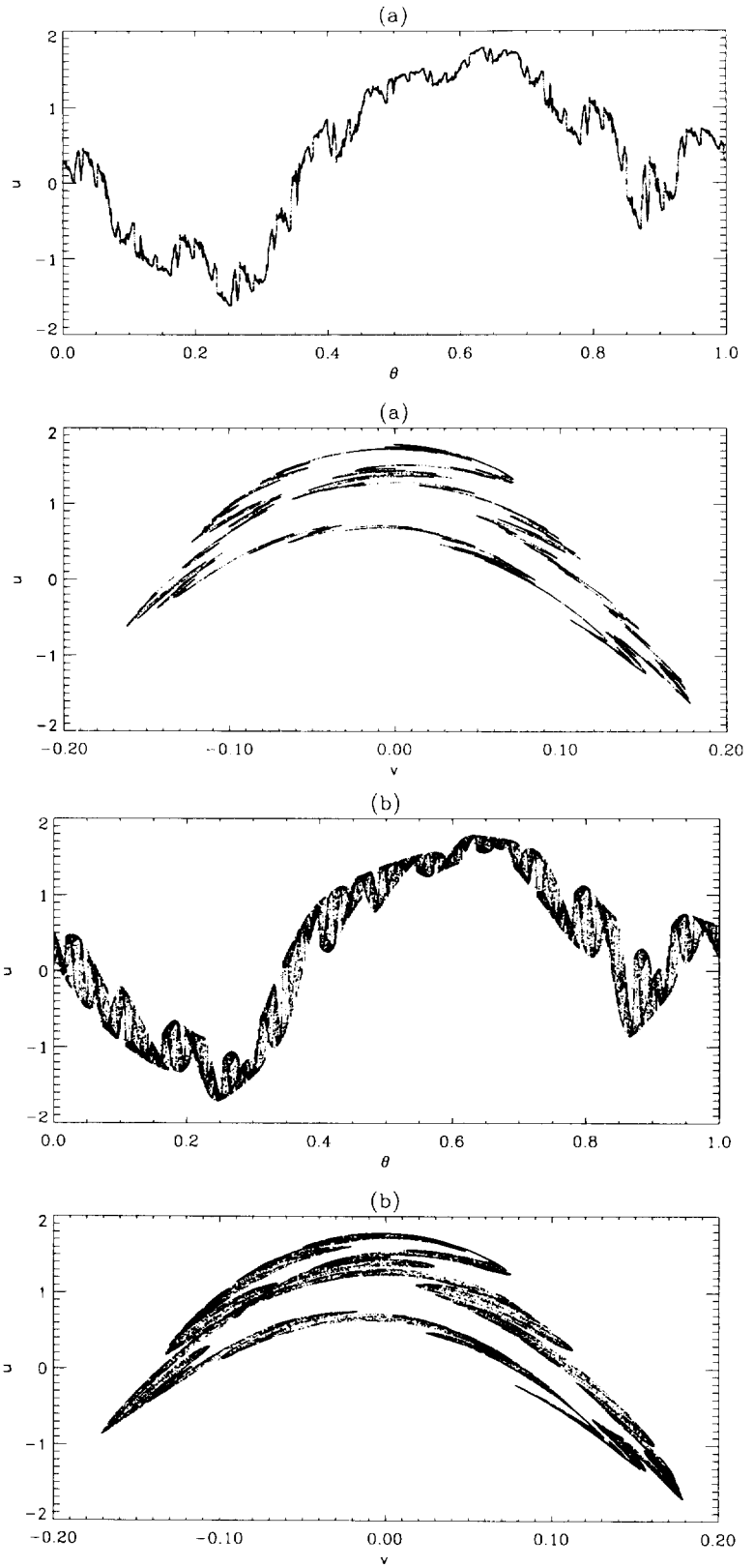

Fig. 1. Projections of phase trajectories for the Hénon map. (a) Nonstrange attractor just below the transition point ($b = 0.68, A = 0.7$); (b) strange nonchaotic attractor ($b = 0.7, A = 0.7$); (c) strange chaotic attractor ($b = 0.77, A = 0.7$).

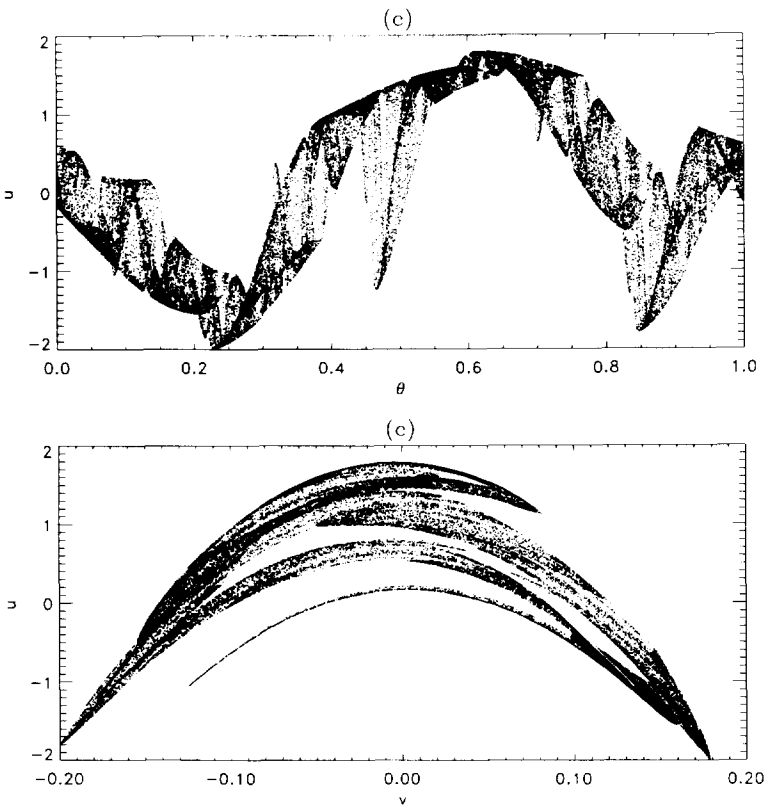

Fig. 1 — continued.

which are directly related to continuous-time models. For this purpose we have to treat two-dimensional mappings instead of one-dimensional ones. Therefore, we must generalize the criteria proposed in Ref. [12] which distinguish strange and nonstrange attractors to higher-dimensional systems (see the Appendix). In Section 2 we introduce the quasiperiodically forced Hénon and ring maps, and give a survey of the behaviour observed in these models without and with forcing. Section 3 is devoted to a detailed analysis of transitions of both maps close to the border of chaos. We show that SNA exists which consist of several bands. Moreover, we report a new type of bifurcation of SNA which resembles the band merging known for chaotic attractors. In this transition the two-band SNA is transformed into a new one-band SNA. We call this a band-merging crisis of SNA. Finally the results are summarized in Section 4.

2. Basic models

We investigate two models which can be considered as prototypes of the transition to chaos through period-doubling and quasiperiodicity. The first model is the Hénon map,

$$u_{n+1} = 1 + v_n - bu_n^2 + A\cos(2\pi\theta_n),$$
$$v_{n+1} = cu_n, \quad \theta_{n+1} = \theta_n + \omega \bmod 1. \tag{1}$$

The second model is the ring map,

$$x_{n+1} = x_n + \Omega - (k/2\pi)\sin(2\pi x_n) + \gamma y_n + A\cos(2\pi\theta_n) \bmod 1,$$
$$y_{n+1} = \gamma y_n - (k/2\pi)\sin(2\pi x_n),$$
$$\theta_{n+1} = \theta_n + \omega \bmod 1. \tag{2}$$

In both mappings a harmonic forcing with amplitude A and frequency ω is included. For rational ω the forcing is periodic, but for irrational ω the forcing is

quasiperiodic. Quasiperiodicity means the presence of at least two incommensurate frequencies, here they are 1 (because of discreteness of time) and ω. The parameters c resp. γ describe dissipation; they give the rate of damping of the phase volume, and should be less than 1. For all computations below these values are fixed at $c = 0.1$ and $\gamma = 0.01$.

In the Hénon map (1) the parameter b is the main bifurcation parameter. In the unforced case $A = 0$, there is a curve in the plane of parameters b, c on which two fixed points (stable and unstable) are born. With increasing b, the transition to chaos via an infinite sequence of period-doubling bifurcations occurs [13].

In the ring map (2) the main bifurcation parameters for $A = 0$ are the nonlinearity k and the phase shift Ω. For small values of the parameter γ, the dynamics of the ring map is similar to that of the circle map. For $k < k_{\text{critical}} \approx 1$ this map has no chaotic trajectories, and its dynamics can be characterized by the rotation number which can be either rational or irrational, corresponding to periodic or quasiperiodic motion. The largest phase-locking intervals survive far beyond k_{critical}, where, as Ω changes, transitions of the type "periodic orbit–chaos" are typically observed.

We discuss now, which qualitative changes appear when the Hénon and the ring maps are forced quasiperiodically. If the amplitude of the forcing is small, it just adds one more frequency to the system. So, a periodic motion becomes a quasiperiodic two-frequency torus and a two-frequency quasiperiodic motion becomes a three-frequency one. With increasing forcing amplitude, a two-frequency torus can become fractal [14], whereas the Lyapunov exponent may remain negative, this means that a SNA appears. In this paper we focus on this transition in both the Hénon and the ring map.

To give an impression of the attractors obtained for different parameter values in systems like (1), (2), we show projections of the phase trajectories for the Hénon map (1) forced quasiperiodically with two different amplitudes. In the plane (θ, u) the two-frequency quasiperiodic motion is presented by an invariant curve (Fig. 1a). This curve can be considered as a cross section (Poincaré map) of a two-frequency torus in a three-dimensional phase space of a continuous-time dynamical system. Therefore, we call this invariant curve a torus in the present paper. For larger forcing amplitude $b = 0.7$ the Lyapunov exponent is still negative but the attractor has a "strange" geometrical structure (Fig. 1b). This attractor is a strange nonchaotic attractor. It is clear that it is difficult to distinguish these two kinds of attractors visually. This can, however, be done with two methods (based on rational approximations resp. phase sensitivity) presented in the Appendix. In the following we call only these attractors SNA if both criteria are fulfilled. If we still increase the forcing the SNA is converted to a strange chaotic attractor with a positive Lyapunov exponent (Fig. 1c).

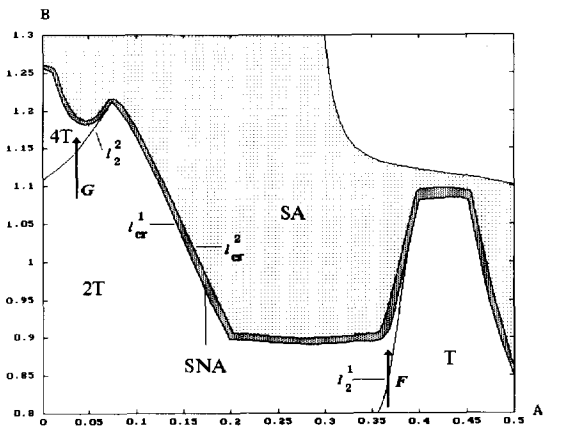

Fig. 2. Bifurcation diagram for the Hénon map.

3. Transitions under quasiperiodic forcing

In this section we discuss the appearance of n-band strange nonchaotic attractors and their transition to chaos.

3.1. Global features of the bifurcation diagram

3.1.1. Hénon map

Fig. 2 shows the bifurcation diagram for the Hénon map in the parameter plane (A, b) for fixed $c = 0.1$. If the external forcing vanishes ($A = 0$), a transition to chaos through an infinite sequence of period-doubling bifurcations occurs. Formally, even for vanishing forcing, the periodic regimes are transformed into two-tori, if the variable θ is taken into account.

For finite A only a finite number of period-doublings is observed, as has been described by Kaneko [14]. Along the line F ($A = 0.36$) we observe only one

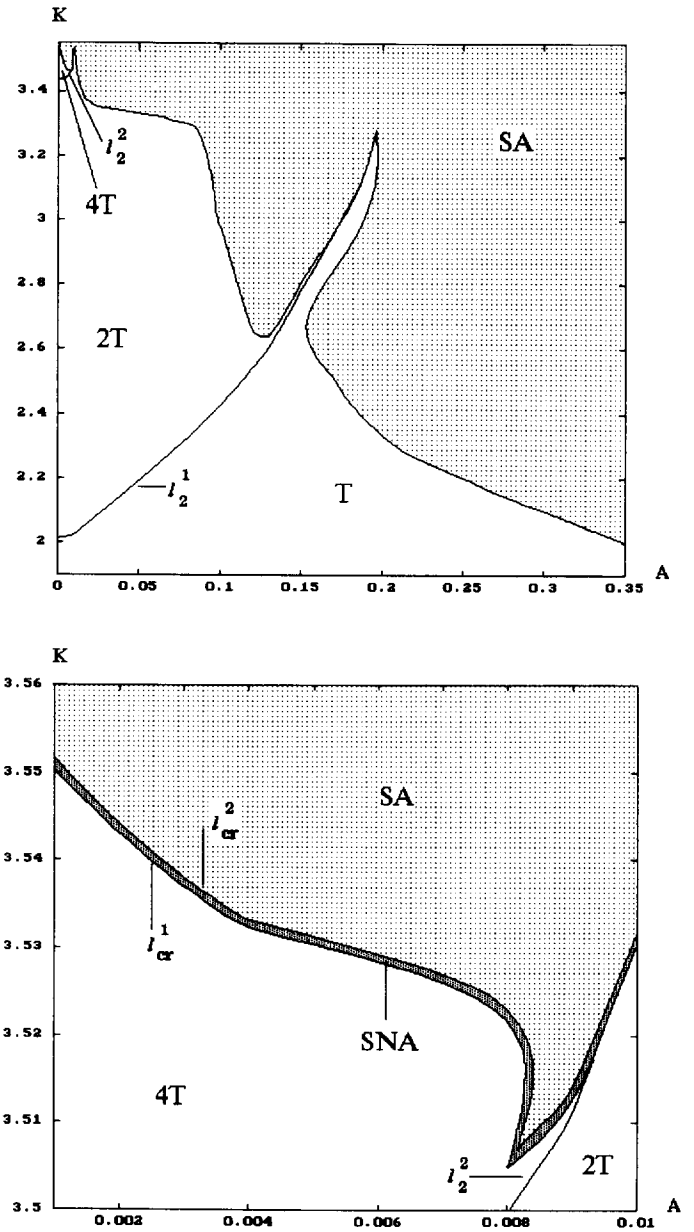

Fig. 3. Bifurcation diagram for the ring map (top panel) and the enlargement of the region near $A = 0, k = 3.55$ (bottom panel).

period-doubling bifurcation of the torus T, but along the direction G ($A = 0.025$) two period-doubling bifurcations of the torus occur before the transition to chaos.

In this case the transition to chaos is accompanied by the loss of smoothness of the torus. In between quasiperiodic motion on the torus and chaos, a strange nonchaotic attractor appears. It exists only in a rather narrow region, as sketched in Fig. 2. The critical curve l_{cr}^2 in Fig. 2 corresponds to the transition from SNA

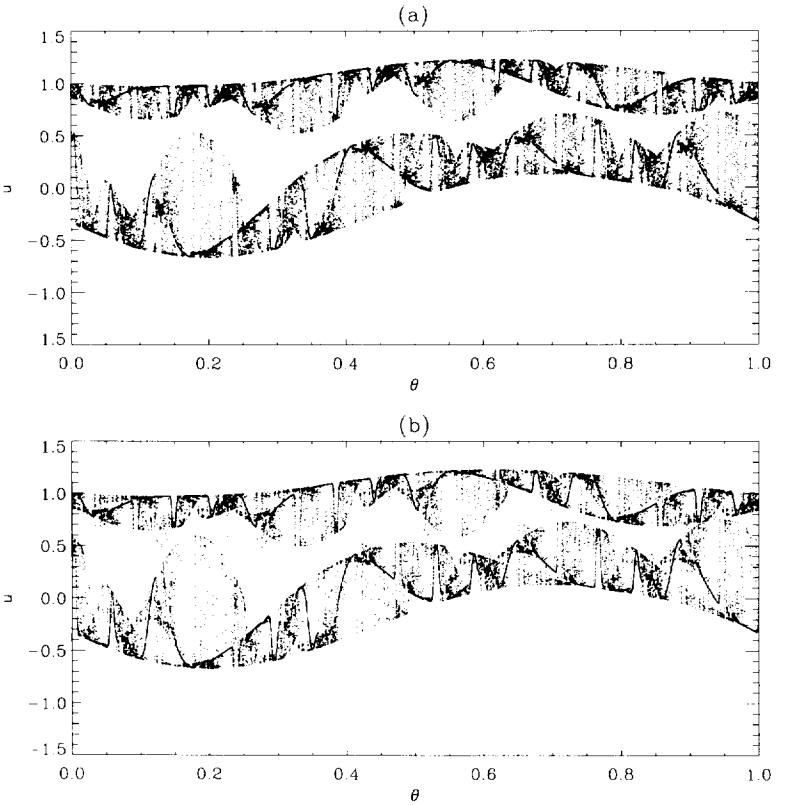

Fig. 4. Hénon map. Projections of phase trajectories (a) for SNA with two bands ($B = 1.03, A = 0.131$) and (b) for SNA with one band appearing as a result of band merging ($B = 1.03, A = 0.1325$).

to chaos. It is determined by the calculation of Lyapunov exponents for different values of the control parameters. At this curve the largest Lyapunov exponent changes its sign. The critical curve l^1_{cr} is the boundary between the smooth torus and SNA which is calculated using the criteria described in the Appendix.

3.1.2. Ring map

Fig. 3 shows the bifurcation diagram for the ring map (2) in the parameter plane (A, k) for fixed $\gamma = 0.01$ and $\Omega = 0$. In this diagram we use the same notations for the torus regimes and for the bifurcation curves as in Fig. 2. This diagram exhibits the same qualitative features as found in the Hénon map: a sequence of period-doublings of tori, transition to chaos, and a SNA between quasiperiodic and chaotic regimes.

3.2. Appearance of n-band SNA

We find for both systems (Figs. 2, 3) new types of SNA: there are SNA with 1, 2 and 4 bands which evolve from the torus, the doubled torus and the quadrupled torus, respectively. Fig. 4a, showing an SNA with 2 bands, illustrates that SNA, similar to chaotic attractors, can be observed also as *banded structures*.

Let us discuss the features of their appearance and their transition to chaos. Up to now we know two mechanisms of the appearance of SNA. Firstly, Heagy and Hammel [5] proposed a mechanism for the appearance of SNA at a band merging crisis of a period-doubled torus with its unstable parent. In this scenario, the SNA is formed at the moment of a crisis as a one-band attractor, and as the nonlinearity parameter increases, a transition from SNA to a chaotic attractor

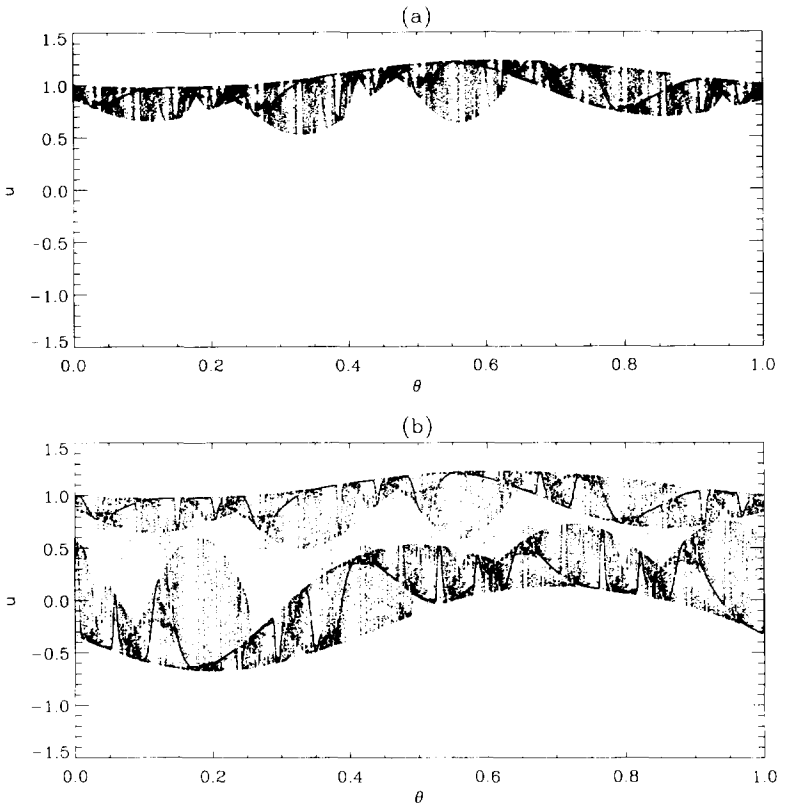

Fig. 5. Plot of each second iteration for the regimes shown in Fig. 4.

is observed. We have also observed this transition to SNA in some parts of the parameter space (for example in some interval around $b = 1.15$ and $A = 0.1$). Secondly, it has been shown for one-band SNA in the quasiperiodically forced circle map that they can appear as a result of a collision of a stable and an unstable torus in a dense set of points [4]. We were not able to obtain this kind of transition for the quasiperiodically forced examples studied in this paper.

However, more typically we find another transition to a banded SNA (Figs. 1, 4a). These banded SNA appear without any collision with an unstable torus, the transition appears to be characterized only by a loss of smoothness of the torus. A similar "fractalization of torus" has been observed in Ref. [14].

It is important to note that the banded structure of the attractor survives after the transition to chaos. When the control parameter changes, the one-band SNA shown in Fig. 1b forms a one-band chaotic attractor (Fig. 1c), and the two-band SNA of the type Fig. 4 evolves to chaos with two bands as well. The same kind of behavior can be observed for the ring map.

3.3. Band merging of SNA

Connected to the appearance of the two-band SNA, we observe another new interesting phenomenon: band-merging of SNA. This phenomenon is similar to that known for strange chaotic attractors, where 2^n bands merge to a larger attractor with 2^{n-1} bands [15]. We demonstrate this transition for the two-band SNA shown in Fig. 4a. By plotting each second iteration (Fig. 5a), it can be checked that the two bands are still separated. With increasing forcing amplitude A, these two bands merge (Figs. 4b, 5b). The corresponding time series also demonstrate a clear difference between the SNA before (Fig. 6a) and

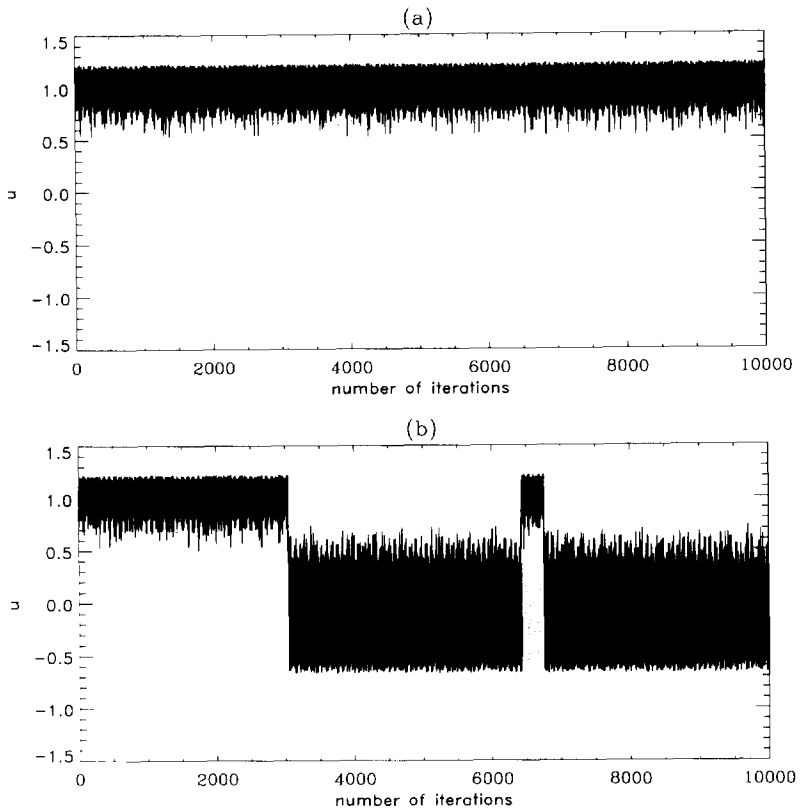

Fig. 6. Time series for the regimes shown in Fig. 4.

after the band merging (Fig. 6b).

It is important to note that the Lyapunov exponents are still negative for parameter values both before and after this merging. This means that the merging of the two bands does not lead to chaos but to a larger one-band SNA. Only further increase of the forcing amplitude A leads to a transition to chaos within this one-band attractor.

We emphasize that this phenomenon of band merging of SNA is a general one. It is observed in both the Hénon map and the ring map. We conjecture that this phenomenon is typical for 2^n-band SNA forming 2^{n-1}-band SNA. For example, Fig. 7 displays band merging for SNA with four bands for the ring map. This merging leads to a two-band SNA which evolves to a two-band chaotic attractor with further increase of the forcing.

4. Summary

We have studied the appearance of SNA and their transition to chaos in quasiperiodically forced maps. The models we used – the Hénon map and the ring map – are diffeomorphisms, and can, therefore, be related to continuous-time models. The existence of SNA in such systems has been checked by two methods: via bifurcation analysis of the rational approximations and by calculating the phase sensitivity. The use of these methods is, in particular, important for high-dimensional maps, because of the difficulties to distinguish between strange and nonstrange nonchaotic attractors only based on visual inspection of phase portraits.

We have shown for the first time that SNA consisting of 2^n bands exist. The appearance of such banded SNA which evolve from n-tori can be regarded as a typical phenomenon for all systems which without

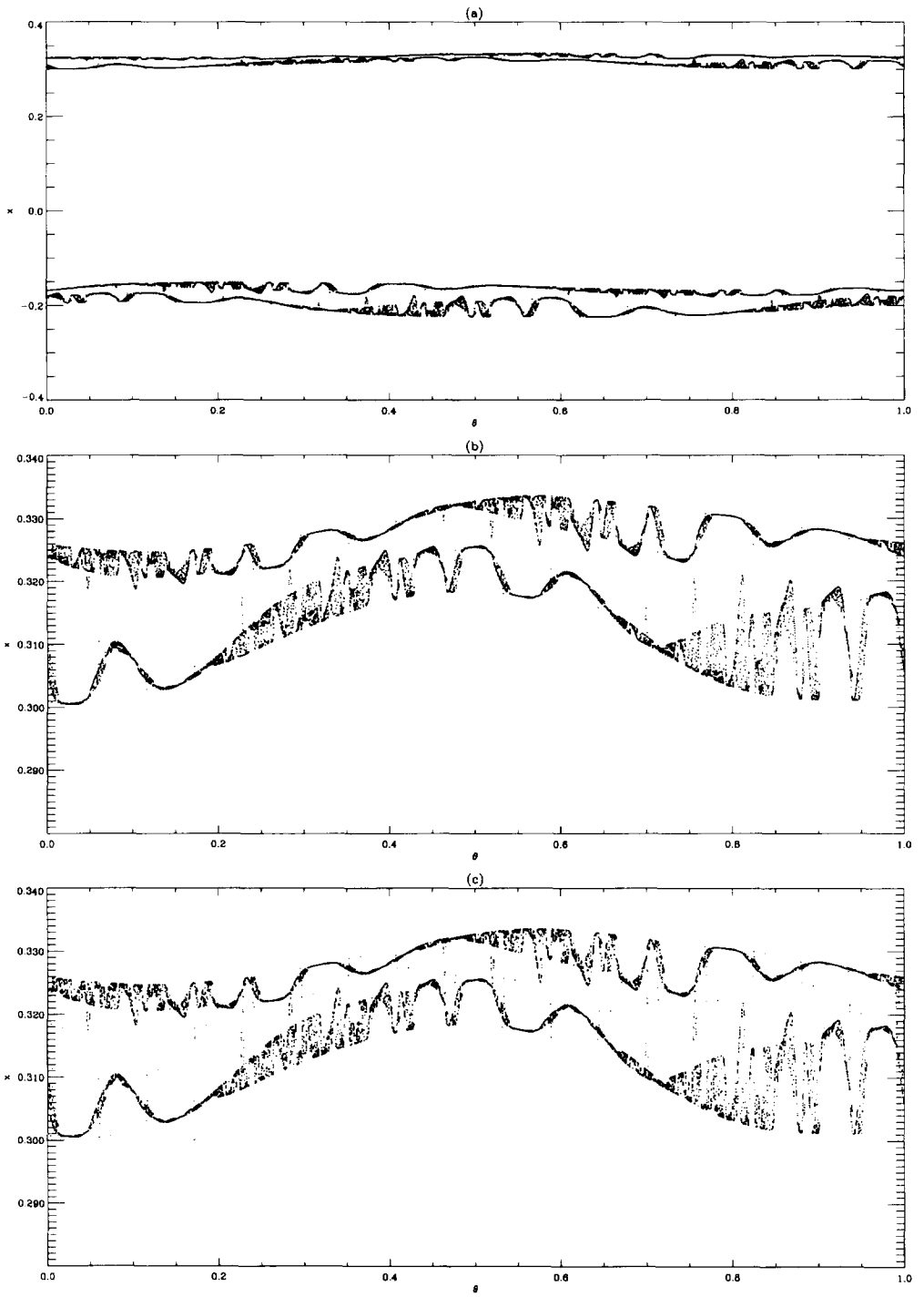

Fig. 7. Ring map. Projections of phase trajectories (a), (b) for SNA with four bands ($k = 3.53, A = 0.00461$) and (c) for SNA with two bands appearing as a result of band merging ($k = 3.53, A = 0.00462$).

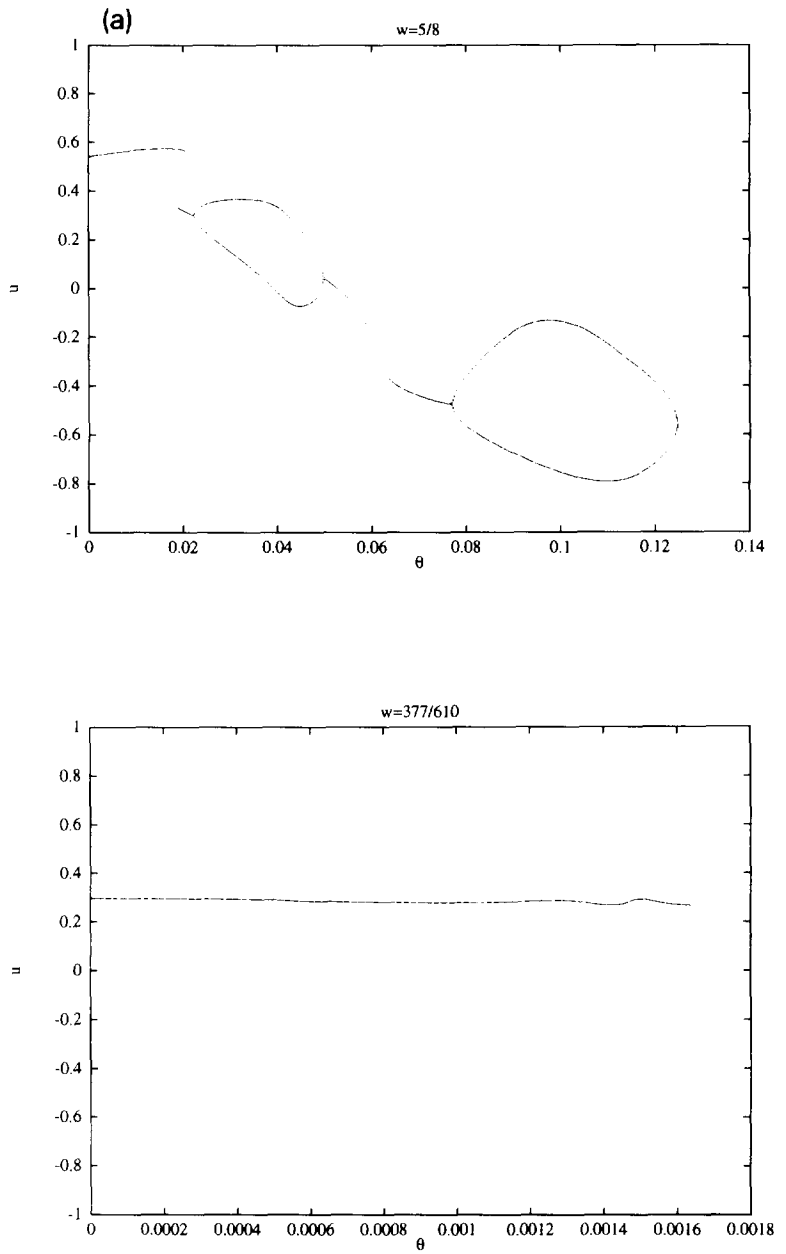

Fig. 8. Bifurcation diagram (a) for the rational approximation $\omega = 5/8$ and $\omega = 377/610$ for a nonstrange attractor and (b) for the strange one shown in Fig. 1.

quasiperiodic forcing possess a period doubling cascade. A detailed study of scaling properties of this transition remains, however, an open question and needs further investigation.

Strongly connected with the occurrence of 2^n-band attractors is the band-merging crisis for SNA. Similar to the chaotic case, a 2^n-band SNA merges to a 2^{n-1}-band SNA. Band merging of SNA occurs mainly as the

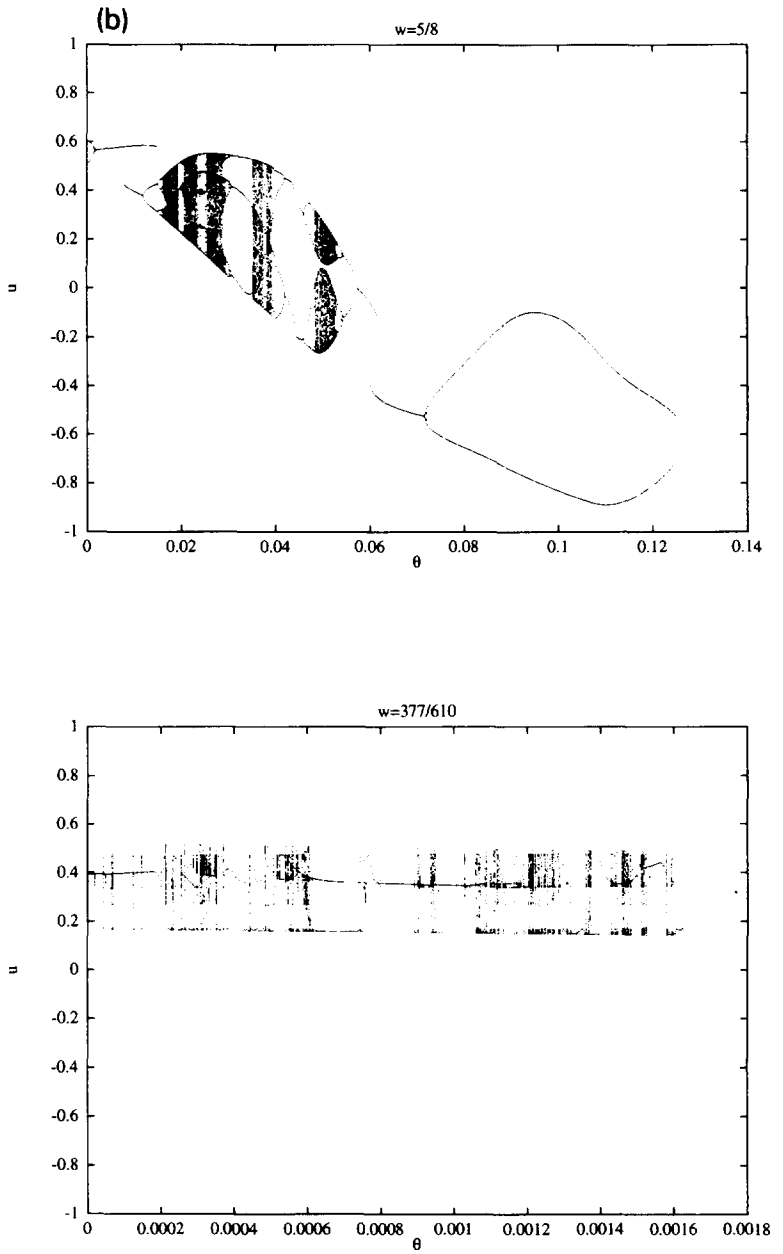

Fig. 8 — continued.

last bifurcation before the transition to chaos and can be, therefore, observed in the vicinity of this transition.

Acknowledgement

We thank C. Grebogi, M. Ding and M. Zaks for useful discussions. O.S. acknowledges support of the Max-Planck-Gesellschaft, the University of Potsdam and the ISF Grant (RNO 000); U.F. thanks the Univer-

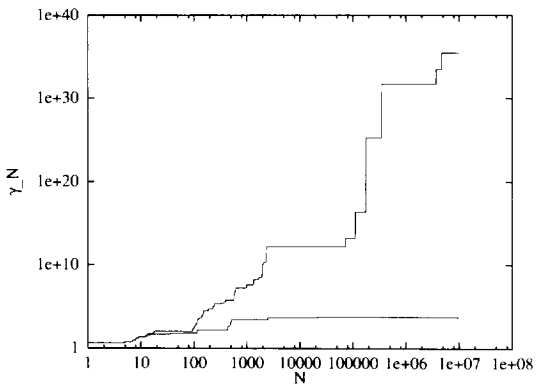

Fig. 9. The maximum of the partial sums $|S_N|$ for a trajectory on the attractors shown in Fig. 1.

sity of Maryland for their hospitality and the DAAD for the financial support of her visit to Maryland.

Appendix A. Characterization of SNA

To verify the existence of a SNA, it is necessary to distinguish between strange and nonstrange attractors. However, direct estimation of the fractal dimension is a very difficult task for such systems [16,17]. Therefore, two special methods have been recently proposed for such a distinction in Ref. [12], where one-dimensional quasiperiodically forced mappings have been studied. The first one is based on the rational approximation of the irrational frequency ω by rationals, the second one considers the sensitivity with respect to the external phase. Below, we generalize these techniques to the higher-dimensional case to apply them to diffeomorphisms.

In general we start from the following equations describing an N-dimensional quasiperiodically forced system,

$$x^i_{n+1} = f_i(x^j_n, \theta_n), \quad i = 1, 2, \ldots, N, \tag{A.1a}$$

$$\theta_{n+1} = \theta_n + \omega \bmod 1, \tag{A.1b}$$

where $f_i(x^j_n, \theta_n)$ are periodic in θ with period 1 and ω is irrational.

A.1. Rational approximations

The first method is based on the bifurcation analysis of the system resulting from periodic approximations of the quasiperiodic forcing. Let us approximate an irrational ω by $\omega_k = p_k/q_k$, where p_k and q_k can be obtained from the continued fraction representation of ω. Throughout this paper we set ω to be the reciprocal of the golden mean: $\omega = (\sqrt{5} - 1)/2$. So, we approximate ω with $\omega_k = F_k/F_{k+1}$, where $F_k = 1, 1, 2, 3, 5, 8, \ldots$ are the Fibonacci numbers. In this case Eq. (A.1b) produces a periodic solution $(\theta_0, \theta_0 + \omega_k, \ldots, \theta_0 + (q_k - 1)\omega_k)$ with period q_k and Eq. (A.1a) is a periodically forced map. The attractor in this map depends on the initial phase θ_0. With continuous variation of the initial phase θ_0 in the interval $[0, 1/F_k]$ we obtain a rational approximation of the attractor in the quasiperiodically forced system.

Since we are interested in the distinction between strange and nonstrange nonchaotic attractors, the smoothness properties of this approximating attracting set are important. For this reason we construct a bifurcation diagram using the initial phase θ_0 as a control parameter. Because (A.1a) is a nonlinear map, different solutions (fixed points, periodic solutions) are possible depending on the initial phase θ_0. Thus, bifurcation points can exist in this diagram. In Ref. [12] it was argued, that if with increasing approximation of ω as $k \to \infty$, one observes bifurcations for sufficiently large p_k and q_k, then the attractor is strange. If there are no bifurcations for sufficiently large p_k and q_k, then the attractor is smooth (nonstrange). For the Hénon map we find that for rational approximations with significantly large F_k (Fig. 8a) there are no bifurcations in case of the attractor shown in Fig. 1a. According to the criterion mentioned above, this means that the attractor is nonstrange. In the case of Fig. 1b the approximating attracting set does indeed possess bifurcations (Fig. 8b). Therefore the quasiperiodically forced Hénon map has a strange nonchaotic attractor for this parameter value.

A.2. Phase sensitivity

In Ref. [12] it was proposed to characterize the attractor's strangeness by calculating a phase sensitivity exponent that measures the sensitivity with respect to changes of phase θ of the external force. From

Eq. (A.1) we easily get recurrence relations for this derivative with respect to the external phase,

$$\frac{\partial \boldsymbol{x}_{n+1}}{\partial \theta} = \frac{\partial \boldsymbol{f}}{\partial \theta} + \boldsymbol{J}(\boldsymbol{x}_n, \theta_n) * \frac{\partial \boldsymbol{x}_n}{\partial \theta}, \tag{A.2}$$

where $\boldsymbol{J}$ is the Jacobian matrix $\boldsymbol{J}(\boldsymbol{x}_l, \theta_l) = \partial f_i(\boldsymbol{x}_l, \theta_l) / \partial x^j$. Starting from some initial derivative $\partial \boldsymbol{x}_0 / \partial \theta$, we get derivatives at all points of the trajectories,

$$\frac{\partial \boldsymbol{x}_{n+1}}{\partial \theta} = \sum_{k=1}^{N} \boldsymbol{R}_{N-k}(\boldsymbol{x}_k, \theta_k) * \boldsymbol{f}_\theta(\boldsymbol{x}_{n-1}, \theta_{n-1}) + \boldsymbol{R}_n(\boldsymbol{x}_0, \theta_0) \frac{\partial \boldsymbol{x}_0}{\partial \theta},$$

where $\boldsymbol{R}_{N-k}(\boldsymbol{x}_k, \theta_k) = \prod_{m=0}^{N-k-1} \boldsymbol{J}(\boldsymbol{x}_{m+k}, \theta_{m+k})$ is the product of the Jacobian matrices and $\boldsymbol{R}_0 = \boldsymbol{I}$, the identity. Because the largest Lyapunov exponent is negative, the last term on the r.h.s. of (A.2) eventually vanishes,

$$\frac{\partial \boldsymbol{x}_N}{\partial \theta} = \boldsymbol{S}_N = \sum_{k=1}^{N} \boldsymbol{R}_{N-k}(\boldsymbol{x}_k, \theta_k) * \boldsymbol{f}_\theta(\boldsymbol{x}_{n-1}, \theta_{n-1}). \tag{A.3}$$

Because the quantity $\boldsymbol{S}_N$ is very intermittent [12], it is more convenient to use

$$\gamma_N^i(\boldsymbol{x}, \theta) = \max_{0<n<N} |S_N^i|. \tag{A.4}$$

If the value of γ_N^i grows with N it means that the x^i as functions of the external phase θ are nondifferentiable, i.e. the attractor is nonsmooth and can be characterized as strange. In the case of smooth attractors this quantity γ_N^i saturates for large N. A SNA is characterized by negative Lyapunov exponents (except the one which is zero), hence, there is no sensitive dependence on initial conditions. But it demonstrates a sensitive dependence with respect to the external phase.

Calculating this derivative with respect to the external phase, we can distinguish the nonstrange attractor in the Hénon map for which γ_N^i (A.4) is bounded (Fig. 9, lower curve) and the strange one for which this quantity is unbounded (Fig. 9, upper curve).

References

[1] C. Grebogi, E. Ott, S. Pelikan and J.A. Yorke, Physica D 13 (1984) 261.
[2] A.S. Pikovsky and U. Feudel, J. Phys. A 15 (1994) 5209.
[3] M. Ding, C. Grebogi and E. Ott, Phys. Rev. A 39 (1989) 2593.
[4] U. Feudel, J. Kurths and A. Pikovsky, Physica D 88 (1995) 176.
[5] J.F. Heagy and S.M. Hammel, Physica D 70 (1994) 140.
[6] F.J. Romeiras and E. Ott, Phys. Rev. A 35 (1987) 4404.
[7] Y.-C. Lai, Phys. Rev. E 53 (1996) 57.
[8] J. Heagy and W.L. Ditto, J. Nonlinear Sci. 1 (1991) 423.
[9] A. Bondeson, E. Ott and T. M. Antonsen, Phys. Rev. Lett. 55 (1985) 2103.
[10] W.L. Ditto, M.L. Spano, H.T. Savage, S.N. Rauseo, J. Heagy and E. Ott, Phys. Rev. Lett. 65 (1990) 533.
[11] T. Zhou, F. Moss and A. Bulsara, Phys. Rev. A 45 (1992) 5394.
[12] A. Pikovsky and U. Feudel, CHAOS 5 (1995) 253.
[13] D.L. Hitzl and F. Zele, Physica D 14 (1985) 305.
[14] K. Kaneko, Collaps of tori and genesis of chaos in dissipative systems (World Scientific, Singapore, 1986).
[15] E. Ott, Chaos in dynamical systems (Cambridge Univ. Press, Cambridge, 1992).
[16] M. Ding, C. Grebogi and E. Ott, Phys. Lett. A 137 (1989) 167.
[17] U. Feudel, M.A. Safonova, J. Kurths and V.S. Anishchenko, Int. J. Bif. Chaos 6, No. 5 (1996).